

Modulated, three-directional, and polar structural instability in layered d^1 NaTiO₂

Alaska Subedi

Centre de Physique Theorique, Ecole Polytechnique, CNRS,
Université Paris-Saclay, F-91128 Palaiseau, France and
Collège de France, 11 place Marcelin Berthelot, 75005 Paris, France

(Dated: June 1, 2021)

I study the experimentally observed metal-to-metal structural phase transition in NaTiO₂ using density functional calculations. I do not find the previously proposed low-temperature structure energetically favorable with respect to the high-temperature rhombohedral structure. The calculated phonon dispersions of the rhombohedral phase show dynamical instabilities at several inequivalent parts of the Brillouin zone, including at the wavevector $(\frac{1}{2}, \frac{1}{5}, \frac{1}{5})$. These instabilities lead to monoclinic structures without inversion symmetry that are modulated along all three directions. The calculated electronic structures show that a local bonding instability of the Ti $3d$ states is associated with the structural transition.

PACS numbers: 64.60.Ej, 63.20.D-, 71.30.+h

I. INTRODUCTION

Layered NaTiO₂ has garnered attention because of its potential as an anode material in sodium-ion batteries.^{1,2} In addition, this material also exhibits a broad metal-to-metal structural transition between 200 and 250 K that has puzzled researchers for more than twenty years.³⁻⁵ Unusual structural transitions are at the heart of several complex phase diagrams, including that of the manganites that show colossal magnetoresistance and the cuprate and iron unconventional superconductors. Unraveling the mechanism of the structural transition in NaTiO₂ and understanding its low temperature phase may illustrate the range of possibilities for structural instabilities in partially filled $3d$ systems. This may also help us understand the causes of structural failures of battery materials, which plague the performance of solid-state batteries.

Above 250 K, NaTiO₂ occurs in a high-symmetry layered rhombohedral structure with space group $R\bar{3}m$.⁶ This α -NaFeO₂-type structure is a modification of the rock-salt structure, and it consists of positive Na⁺/Ti³⁺ and negative O²⁻ ions at the sites of two interpenetrating fcc lattices, with the NaO₆ and TiO₆ octahedra alternating along the rock-salt [111] direction. Within each layer, the octahedra share edges so that Na⁺/Ti³⁺ ions make equilateral triangles. In the out-of-plane direction, the NaO₆ octahedra are elongated with respect to the in-plane distances, while the TiO₆ octahedra are compressed. As a consequence, the Na⁺ and Ti³⁺ ions are in antiprismatic ($\bar{3}m$), rather than octahedral ($m\bar{3}m$), coordination.

NaTiO₃ formally contains d^1 Ti³⁺ ions with spin $S = \frac{1}{2}$ arranged in a triangular lattice. The initial interest in this material came from the possibility of realizing a resonating valence bond state of spin singlet pairs as suggested by Anderson.⁷⁻¹⁰ Experimentally, however, this material is metallic and shows a small, almost temperature independent magnetic susceptibility above 250 K.³⁻⁵ As the temperature is lowered, signatures of a broad

phase transition are seen in neutron diffraction, magnetic susceptibility, and heat capacity experiments. Several diffraction peaks of the high-temperature rhombohedral structure split during the phase transition, and the low-temperature structure has been resolved by Clarke *et al.* to be in space group $C2/m$ with shortened Ti-Ti bonds.^{4,5} This continuous phase transition is not accompanied by a smooth change in the Ti-Ti bond lengths. Instead, the rhombohedral and monoclinic phases with different bond lengths coexist over the temperature range of the transition, and the fraction of the monoclinic phase progressively increases as the temperature is lowered. The magnetic susceptibility decreases continuously between 250 and 200 K, remains almost constant until 100 K, and then starts to rise again, presumably due to impurities, as the temperature is further lowered. Heat capacity measurements show a peak near 260 K, which provides an unmistakable evidence for a bulk phase transition. None of the aforementioned measurements exhibit any hysteresis behavior.

The metal-to-metal transition in NaTiO₂ has been described in terms of increased bandwidth due to stronger Ti-Ti bonds.⁵ This picture relies on an electronic instability that lifts the orbital degeneracy of the d^1 Ti³⁺ electron. Several theoretical studies have studied the electronic properties of NaTiO₂ and tried to identify a mechanism for such an instability,¹¹⁻¹⁵ but the microscopic basis for the phase transition has still not been fully clarified.

In this paper, I reexamine the metal-to-metal structural phase transition observed in NaTiO₂ using density functional calculations. I do not find the experimentally proposed low-temperature structure energetically favorable compared to the high-temperature rhombohedral structure. However, the calculated phonon dispersions of the rhombohedral phase do show dynamical instabilities at several inequivalent places in the Brillouin zone. The structural distortions corresponding to the unstable phonon modes cause modulations along both in-plane and out-of-plane directions and lead to a mon-

oclinic phase without inversion symmetry. The wavevectors of the unstable phonons do not nest the Fermi sheets. Hence, the monoclinic phase cannot be characterized as a charge-density-wave state. Instead, I find that the transition is due to a local bonding instability of the partially filled Ti 3*d* states.

II. COMPUTATIONAL DETAILS

The results presented here were obtained from calculations based on density functional theory within the local density approximation. The structural and magnetic relaxations were performed using the pseudopotential-based planewave method as implemented in the Quantum ESPRESSO package. The phonon dispersions were calculated using density functional perturbation theory.¹⁶ The cut-offs were set to 50 and 500 Ryd for the basis-set and charge-density expansions, respectively. The pseudopotentials generated by Garrity *et al.* were used in these calculations.¹⁷ I used a $14 \times 14 \times 14$ grid for Brillouin zone sampling, and equivalent or denser grids were used in the supercell calculations. The dynamical matrices were calculated on an $8 \times 8 \times 8$ grid, and the phonon dispersions were obtained by Fourier interpolation. All the results presented in this paper were calculated using the fully relaxed structures in the respective phases. Some calculations were also performed using the general full-potential linearized augmented planewave method as implemented in the WIEN2K package.¹⁸

The phonon frequencies except the unstable branch are converged to less than a percent with the above cut-offs and grids, and a Marzari-Vanderbilt smearing of 0.02 Ryd.¹⁹ The unstable branch was not converged even when using a computationally-demanding *k*-point grid of $18 \times 18 \times 18$, and I let it be because the unstable frequencies cannot be measured anyway. I confirmed the presence of the structural instability by stabilizing supercell structures that are distorted according to the unstable phonons. A drawback for not converging the unstable branch is that I am not fully sure of the wavevector that has the strongest instability.

III. RESULTS AND DISCUSSIONS

Several theoretical studies based on both first principles and model calculations have attempted to clarify the instability in NaTiO₂ that leads to the low-temperature *C2/m* structure proposed by Clarke *et al.*^{11–15} Instead of trying to search for the mechanism that leads to the proposed low-temperature phase, I started my investigation by trying to stabilize the experimentally determined structure. However, when I fully relaxed the experimental *C2/m* structure, it relaxed to the high-temperature rhombohedral structure with *R3m* symmetry. This was true regardless of whether I allowed a magnetic solution or not. Even if I started with a magnetically ordered state

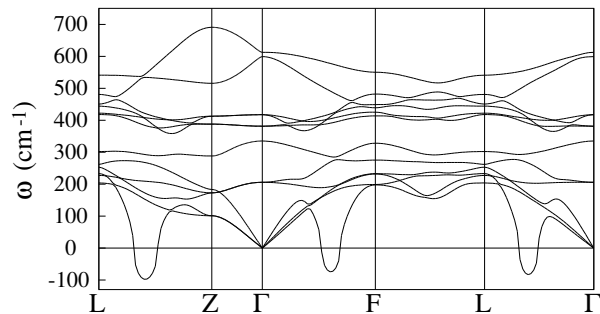


FIG. 1. Calculated phonon dispersions of NaTiO₂ in the rhombohedral structure with space group *R3m*. The dispersions are plotted along the path $L (\frac{1}{2}, 0, 0) \rightarrow Z (\frac{1}{2}, \frac{1}{2}, \frac{1}{2}) \rightarrow \Gamma (0, 0, 0) \rightarrow F (\frac{1}{2}, \frac{1}{2}, 0) \rightarrow L (\frac{1}{2}, 0, 0) \rightarrow \Gamma (0, 0, 0)$ in the Brillouin zone of the primitive unit cell. The imaginary frequencies are represented with negative values.

TABLE I. The eigendisplacement vector of the unstable phonon mode of rhombohedral NaTiO₂ at the wavevector $(\frac{1}{2}, \frac{1}{5}, \frac{1}{5})$.

atom	<i>x</i>	<i>y</i>	<i>z</i>
Na	$-0.024 + 0.012i$	$0.042 - 0.022i$	$0.112 - 0.057i$
Ti	$0.248 - 0.250i$	$-0.430 + 0.432i$	$-0.062 + 0.063i$
O	$0.037 + 0.052i$	$-0.065 - 0.090i$	$0.002 + 0.472i$
O	$-0.052 - 0.037i$	$0.090 + 0.064i$	$-0.472 + 0.000i$

with large initial moments, the system relaxed to the rhombohedral structure with no or very small moments. This lack of a strong magnetic instability is consistent with the experiments, which show almost temperature independent magnetic susceptibility with a small value of $\chi \approx 4.5 \times 10^{-4}$ emu/mol for the high-temperature phase.^{3,5}

I calculated the phonon dispersions of rhombohedral NaTiO₂ in the theoretical structure to examine if this material has any dynamical instabilities as suggested by the experiments. The relaxed rhombohedral unit cell has the hexagonal lattice parameters of $a = 2.9235$ and $c = 16.2167$ Å and the internal O parameter of $z = 0.2370$. The phonon dispersions, shown in Fig. 1, do not display any instabilities at or near the Brillouin zone center. In particular, the acoustic branches do not exhibit any softness even along the Cartesian *z* direction $\Gamma \rightarrow Z$ (*i.e.* the rhombohedral [111] direction). In fact, the acoustic branch that is polarized along the out-of-plane direction has the largest dispersion. This demonstrates the presence of strong interlayer bonding despite the layered structure of this material.

A conspicuous feature in the phonon dispersions is the presence of a phonon branch that is unstable along the *L*–*Z*, Γ –*F* and *L*– Γ paths. I find that the largest instability is at the wavevector $(\frac{1}{2}, \frac{1}{5}, \frac{1}{5})$ in terms of the primitive reciprocal lattice vectors of the rhombohedral cell. The atomic displacements corresponding to this wavevector

occur along all three directions, and it is remarkable that a three-directional structural instability could occur for a layered material. The unstable phonon mode has an irreducible representation A' of the point group m , which is a subgroup of the point group $\bar{3}m$ of the high-temperature structure. This implies that the distortions corresponding to the unstable mode leads to a structure with a point group symmetry m . This is a crystal class without inversion symmetry. The eigendisplacement vector of this unstable mode is given in Table I. As one can see, this mode causes displacements of all four atoms of the rhombohedral unit cell. The loss of inversion symmetry is also evident from the asymmetric displacement pattern of the cations relative to that of the negatively charged O^{2-} .

I performed full structural relaxations of 200-atom $2 \times 5 \times 5$ supercells to be certain that the structural instability is real. When the starting structure consisted of a supercell with randomly displaced atomic positions of the high-temperature structure, the relaxation converged back to the high-symmetry rhombohedral structure. However, when I started with a supercell that had atoms displaced according to the displacement pattern obtained from the eigendisplacement vector of the unstable mode, the relaxation yielded a lower-symmetry structure whose total energy was only ~ 1.4 meV/atom lower than that of the rhombohedral structure. The changes in bond lengths due to the structural distortions are relatively small. The Na-O and Ti-O bond lengths change by between 0.001 to 0.135 Å (corresponding to changes of 0.05–6.0%), which encompasses the range of 0.5–1.5% changes in bond lengths experimentally determined by Clarke *et al.* However, the distortion pattern of the NaO_6 and TiO_6 octahedra is complex, owing to the wavevector $(\frac{1}{2}, \frac{1}{5}, \frac{1}{5})$ corresponding to the instability that repeats the distortions over a comparatively large distance. The low-symmetry structure can be refined to a ten formula unit (40 atoms) monoclinic unit cell with space group Cm , and the full structural information is given in Table II in the Appendix. Note that this structure lacks inversion symmetry. However, the off-centerings of the cations in the oxygen cages are small, and the structure can also be refined to $C2/m$ symmetry if the tolerance in the symmetry finder code is increased to 0.03 Å. Therefore, the results of my structural relaxations are not completely inconsistent with Clarke *et al.*'s experiment that resolves the low-temperature structure to the space group $C2/m$. The volume of my low-symmetry structure is same as that of the high-symmetry structure, again in agreement with the experiment.

Similar dynamical instabilities occur at other points in the Brillouin zone of the rhombohedral unit cell, and I also performed structural relaxations of a 12-atom $1 \times 1 \times 3$ supercell. Again, the supercell relaxed to a low-symmetry Cm structure when the starting structure consisted of distortions according to the eigendisplacement vector of the unstable mode at the wavevector $(0, 0, \frac{1}{3})$. The total energy of this low-symmetry structure is ~ 0.9 meV/atom lower than that of the high-symmetry

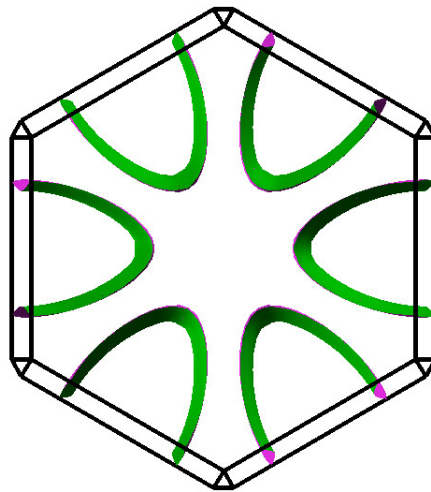


FIG. 2. (Color online) Calculated Fermi surface of rhombohedral $NaTiO_2$.

rhombohedral structure. The total energies of the low-symmetry structures due to dynamical instabilities at wavevectors $(\frac{1}{2}, \frac{1}{5}, \frac{1}{5})$ and $(0, 0, \frac{1}{3})$ are so close, and the distortions so similar (both phonons belong to the A' irreducible representation of the point group m), that the distortions due to these instabilities could coexist below the transition temperature. It is worth emphasizing that the experimentally observed phase transition in $NaTiO_2$ is continuous. The picture of a structural phase transition caused by finite-wavevector phonon instabilities that lead to low-symmetry structures that are almost degenerate in energy is consistent with this experimental evidence.

What might be the cause of this phase transition? The usual suspect for the cause of a finite-wavevector structural distortion is charge density wave instability due to a Fermi surface nesting. I studied the electronic structure of rhombohedral $NaTiO_2$ to investigate the possibility of this instability. The calculated Fermi surface of this material is shown in Fig. 2, and it consists of fairly two-dimensional elliptical cylinders that cross the six faces of the Brillouin zone boundary. Since the Fermi sheets are elliptical, there are no pronounced nestings. Furthermore, the stable phonon branches do not show any Kohn anomalies at the wavevectors corresponding to the imaginary phonon frequencies. Therefore, a charge density wave instability cannot be the cause of the structural phase transition experimentally observed in this material.

A comparison of the electronic structures of rhombohedral and monoclinic $NaTiO_2$ also gives further evidence that the structural transition is not related to the instability of the Fermi surface. The calculated electronic density of states (DOS) of the two phases are shown in Fig. 3, and it shows that electronic states over a wide range of energy are modified. This is in contrast to a

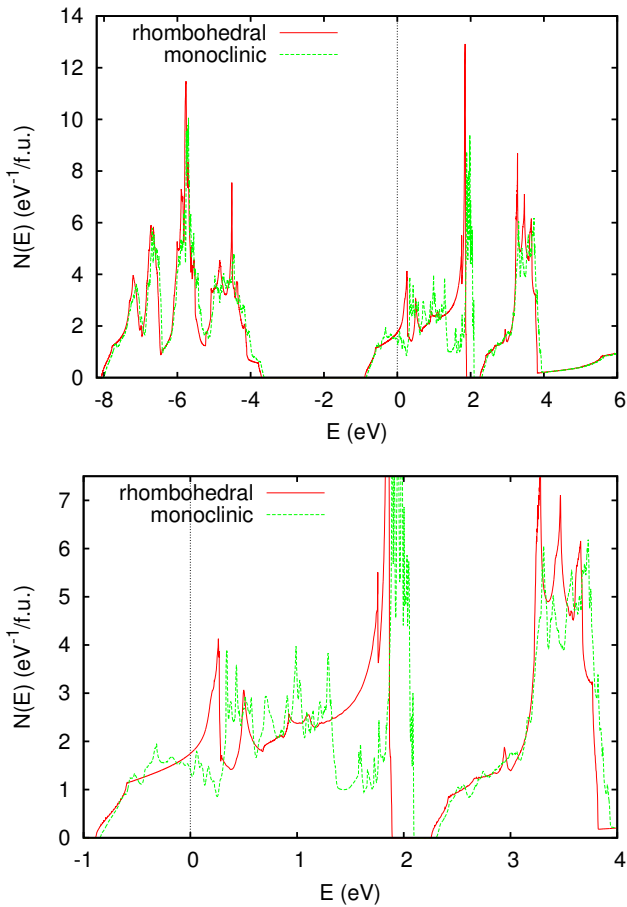


FIG. 3. (Color online) Calculated electronic density of states of rhombohedral and monoclinic NaTiO_2 . The monoclinic structure refers to the distortion due to the $(\frac{1}{2}, \frac{1}{5}, \frac{1}{5})$ phonon instability. The lower panel is a blowup of the Ti $3d$ manifold.

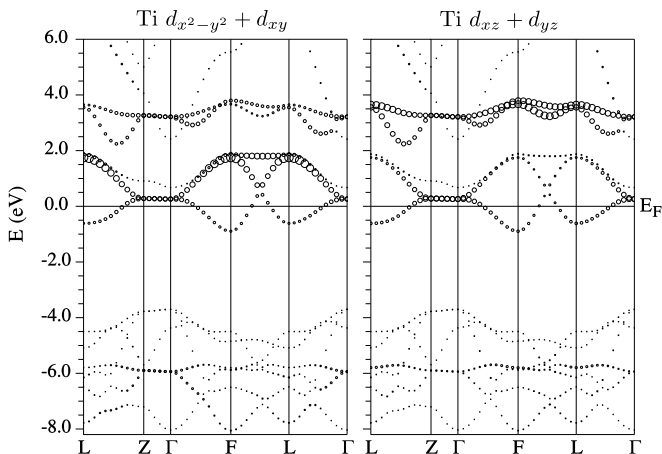


FIG. 4. Calculated band structures of rhombohedral NaTiO_2 plotted with circles of size proportional to the Ti $d_{x^2-y^2} + d_{xy}$ (left) and Ti $d_{xz} + d_{yz}$ (right) characters. The orbitals are defined in the Cartesian coordinates of the conventional unit cell.

charge density wave instability, which would only change electronic states near the Fermi energy. I do find that the DOS at the Fermi level is reduced from 1.75 eV^{-1} per formula unit in the rhombohedral phase to 1.41 eV^{-1} per formula unit in the monoclinic cell due to the $(\frac{1}{2}, \frac{1}{5}, \frac{1}{5})$ phonon instability, a reduction of 19%. However, unlike in a charge density wave transition, where one would observe an increase in the density of states immediately above the charge density wave-induced gap, there is actually a large decrease and redistribution of DOS immediately above the Fermi energy.

The electronic states between -8.10 and -3.60 eV have dominant O $2p$ character. As the band structure of the rhombohedral phase plotted in Fig. 4 shows, these states also exhibit some Ti $3d$ character, and this reflects the formally bonding O $2p$ -Ti $3d$ nature of these states. The states between -0.90 and 3.85 eV show mostly Ti $3d$ character, and these are formally antibonding. The Fermi energy corresponds to this manifold being occupied by one electron. In the point group $\bar{3}m$ of the rhombohedral phase, the five Ti $3d$ orbitals can be grouped into states with irreducible representations e_g and a_{1g} . There are two sets of e_g states in this point group, namely $(d_{x^2-y^2}, d_{xy})$ and (d_{xz}, d_{yz}) . Nominally, the upper Ti $3d$ manifold consisting of two bands between 2.25 and 3.85 eV would correspond to the d_{xz} and d_{yz} states, and the lower two bands in the lower manifold would be $d_{x^2-y^2}$ and d_{xy} states. However, there is significant mixing of orbital characters between the two manifolds due to hopping—either direct or via O $2p$ orbitals—between neighboring Ti ions. In addition, the nominally a_{1g} band with dominant d_{z^2} character that lies in the upper part of the lower Ti $3d$ manifold also shows $d_{x^2-y^2}$ and d_{xy} characters, and the lower e_g manifold correspondingly shows a noticeable d_{z^2} character. This mixing of $3d$ orbitals in this structure type has also been emphasized in the context of $R\bar{3}m$ NaCoO_2 .^{20–22} Therefore, the narrow e_g manifold crossing the Fermi level should not be viewed as being strongly correlated due to the effect of a large on-site Coulomb repulsion U . The effective U for the orbitals corresponding to this manifold should be strongly reduced because these orbitals would be quite extended with large tails not only at O sites, but also at neighboring Ti ions when other manifolds are integrated out. However, this is not to say that the calculated bandwidth will not be renormalized, and it would be interesting to perform beyond density functional theory calculations to study the effects of correlations.

Coming back to Fig. 3, it is striking to note that small differences in the atomic positions between the rhombohedral and monoclinic phases cause a large reconstruction of the electronic structure. The peak at 0.26 eV above the Fermi energy in the rhombohedral phase, which is formed by states with mixed $d_{xz}, d_{yz}, d_{x^2-y^2}$, and d_{xy} characters, collapses in the monoclinic phase. Similarly, the peak in the DOS near the upper edge of the lower e_g manifold that is made out of states with d_{z^2} character moves higher in energy in the monoclinic

phase. These peaks are caused by the narrow dispersion of the bands in the out-of-plane direction, and it reflects the layered nature of this material. The large changes in the shapes and positions of these peaks establish that the Ti 3*d* states and changes in the effective hybridization in the out-of-plane direction play a key role in the structural transition.

The shape of the DOS curve changes greatly due to the structural transition, but there is in fact little change in the bandwidths of the O 2*p* or Ti 3*d* manifolds. The bandwidth of the Ti 3*d* manifold increases by 0.1 eV, which is small compared to its overall bandwidth of 4.75 eV. The gap between the two *e_g* manifolds, which is 0.38 eV in the rhombohedral phase, shows a larger change and decreases to 0.22 eV in the monoclinic phases. This again indicates the importance of effective Ti-Ti interaction for the structural instability. The comparatively small role of Ti-O bonding in the transition is supported by the relatively minor changes in the shape and position of the O 2*p* manifold. The Na electronic states, which lie above 4 eV relative to the Fermi energy, show almost no change. This indicates that Na ions play an insignificant role in the structural instability.

Although NaTiO₂ is a rare example of a system that exhibits a finite-wavevector modulated structural distortions due to a local (in the sense of pertaining to immediate neighbors) bonding instability, it is not the only material that shows such an instability. The transition to a modulated structure observed in IrTe₂ has also been described in terms of a local bonding instability associated with the Te 5*p* states.^{23,24} NaTiO₂ illustrates that such a local instability can also occur in transition metal oxides with partially filled 3*d* orbitals.

IV. SUMMARY AND CONCLUSIONS

In conclusion, I have found that modulated structural distortions occur in *d*¹ NaTiO₂. These distortions occur in all three directions and are different from those previously reported for the low-temperature experimen-

tal structure. The structural distortions correspond to unstable phonon modes that are nominally polar in nature. The unstable phonon modes occur at several inequivalent parts of the Brillouin zone. I relaxed 200-atom and 12-atom supercells corresponding to the instabilities at the wavevectors $(\frac{1}{2}, \frac{1}{5}, \frac{1}{5})$ and $(0, 0, \frac{1}{3})$, respectively, and found that noncentrosymmetric monoclinic structures with space group *Cm* are stabilized. These structures are lower in energy by only 1.4 and 0.9 meV/atom, respectively, than the high-temperature rhombohedral phase. Such a small energy difference is consistent with the continuous nature of the phase transition observed in this material. The phonon instabilities do not correspond to any Fermi surface nestings, and the structural instability cannot be described as being of the charge density wave type. The distortions are due to a local bonding instability of the Ti 3*d* states, which changes the electronic structure over a wide range of energy. Similar bonding instability associated with the Te 5*p* states has been discussed in IrTe₂. The results discussed here show that such an instability can also occur in a partially filled 3*d* system.

ACKNOWLEDGMENTS

I am grateful to Gwen elle Rouse for helpful discussions. This work was supported by the European Research Council grants ERC-319286 QMAC and ERC-61719 CORRELMAT and the Swiss National Supercomputing Center (CSCS) under project s575.

Appendix A: Structure

The full structural details of the structures corresponding to the phonon instabilities at the wavevectors $(\frac{1}{2}, \frac{1}{5}, \frac{1}{5})$ and $(0, 0, \frac{1}{3})$ are given in Tables II and III, respectively. These were obtained by first fully relaxing the respective $2 \times 5 \times 5$ and $1 \times 1 \times 3$ supercells, and then refining thus obtained structure using the FINDSYM code.²⁵

¹ A. Mazzaz, C. Delmas, and P. Hagenmuller, *J. Inclusion Phenom.* **1**, 45 (1983).
² D. Wu, X. Li, B. Xu, N. Twu, L. Liu, and G. Ceder, *Energy Environ. Sci.* **8**, 195 (2015).
³ K. Takeda, K. Miyake, K. Takeda, and K. Hirakawa, *J. Phys. Soc. Jpn.* **61**, 2156 (1992).
⁴ S. J. Clarke, A. C. Duggan, A. J. Fowkes, A. Harrison, R. M. Ibberson, and M. J. Rosseinsky, *Chem. Commun.* **3**, 409 (1996).
⁵ S. J. Clarke, A. J. Fowkes, A. Harrison, R. M. Ibberson, and M. J. Rosseinsky, *Chem. Mater.* **10**, 372 (1998).
⁶ P. Hagenmuller, A. Lecerf, and M. Onillon, *C. R. Acad. Sci* **255**, 928 (1962).

⁷ P. W. Anderson, *Mater. Res. Bull.* **8**, 153 (1973).
⁸ P. Fazekas and P. W. Anderson, *Philos. Mag.* **30**, 423 (1974).
⁹ K. Hirakawa, H. Kadowaki, and K. Ubukoshi, *J. Phys. Soc. Jpn.* **54**, 3526 (1985).
¹⁰ I. Yamada, K. Ubukoshi, and K. Hirakawa, *J. Phys. Soc. Jpn.* **54**, 3571 (1985).
¹¹ H. F. Pen, J. van den Brink, D. I. Khomskii, and G. A. Sawatzky, *Phys. Rev. Lett.* **78**, 1323 (1997).
¹² S. Y. Ezhov, V. I. Anisimov, H. F. Pen, D. I. Khomskii, and G. A. Sawatzky, *Europhys. Lett.* **44**, 491 (1998).
¹³ D. I. Khomskii and T. Mizokawa, *Phys. Rev. Lett.* **94**, 156402 (2005).

TABLE II. Atomic positions of the fully-relaxed monoclinic structure with Cm space group corresponding to the unstable phonon mode at $(\frac{1}{2}, \frac{1}{5}, \frac{1}{5})$. The lattice parameters are $a = 24.4313$, $b = 2.9241$, $c = 11.3368$ Å, $\alpha = 90^\circ$, $\beta = 98.8352^\circ$, and $\gamma = 90^\circ$.

atom	x	y	z
Na	0.00049	0.00000	-0.00117
Na	0.40066	0.00000	0.39881
Na	0.79993	0.00000	0.80004
Na	0.19929	0.00000	0.20135
Na	0.59962	0.00000	0.60096
Na	-0.00048	0.00000	0.50067
Na	0.39931	0.00000	-0.09847
Na	0.80007	0.00000	0.29980
Na	0.20073	0.00000	0.69843
Na	0.60037	0.00000	0.09957
Ti	0.89817	0.00000	0.64883
Ti	0.29624	0.00000	0.04763
Ti	0.69924	0.00000	0.44956
Ti	0.10305	0.00000	0.85188
Ti	0.50314	0.00000	0.25193
Ti	-0.09862	0.00000	0.15079
Ti	0.30385	0.00000	0.55238
Ti	0.70107	0.00000	-0.04930
Ti	0.09650	0.00000	0.34788
Ti	0.49735	0.00000	0.74842
O	-0.04771	0.00000	0.30514
O	0.35249	0.00000	0.71218
O	0.75242	0.00000	0.11283
O	0.15297	0.00000	0.50731
O	0.55329	0.00000	-0.09689
O	-0.04739	0.00000	0.81022
O	0.35326	0.00000	0.20453
O	0.75284	0.00000	0.60314
O	0.15223	0.00000	0.00856
O	0.55246	0.00000	0.41363
O	0.84698	0.00000	-0.00296
O	0.24681	0.00000	0.39472
O	0.64749	0.00000	0.78899
O	0.04751	0.00000	0.18660
O	0.44781	0.00000	0.59258
O	0.84758	0.00000	0.48666
O	0.24756	0.00000	0.88865
O	0.64758	0.00000	0.29564
O	0.04669	0.00000	0.69667
O	0.44714	0.00000	0.09180

- ¹⁴ M. Dhariwal, T. Maitra, I. Singh, S. Koley, and A. Taraphder, Solid State Commun. **152**, 1912 (2012).
- ¹⁵ M. Dhariwal, L. Pisani, and T. Maitra, J. Phys.: Condens. Matter **26**, 205501 (2014).
- ¹⁶ S. Baroni, S. de Gironcoli, A. Dal Corso, and P. Giannozzi, Rev. Mod. Phys. **73**, 515 (2001).
- ¹⁷ K. F. Garrity, J. W. Bennett, K. M. Rabe, and D. Vanderbilt, Comp. Mater. Sci. **81**, 446 (2014).
- ¹⁸ P. Blaha, K. Schwarz, G. Madsen, D. Kvasnicka, and J. Luitz, "WIEN2k, An Augmented Plane Wave + Local Orbitals Program for Calculating Crystal Properties" (K. Schwarz, Tech. Univ. Wien, Austria) (2001).
- ¹⁹ N. Marzari, D. Vanderbilt, A. De Vita, and M. C. Payne, Phys. Rev. Lett. **82**, 3296 (1999).
- ²⁰ M. D. Johannes, D. A. Papaconstantopoulos, D. J. Singh, and M. J. Mehl, Erophys. Lett. **68**, 433 (2004).
- ²¹ S. Landron and M. B. Lepetit, Phys. Rev. B **74**, 184507 (2006).
- ²² S. Landron and M. B. Lepetit, Phys. Rev. B **77**, 125106 (2008).
- ²³ A. F. Fang, G. Xu, T. Dong, P. Zheng, and N. L. Wang, Nat. Sci. Rep. **3**, 1153 (2013).
- ²⁴ H. Cao, B. C. Chakoumakos, X. Chen, J. Yan, M. A. McGuire, H. Yang, R. Custelcean, H. Zhou, D. J. Singh, and D. Mandrus, Phys. Rev. B **88**, 115122 (2013).
- ²⁵ H. T. Stokes and D. M. Hatch, J. Appl. Cryst. **38**, 237-238 (2005).

TABLE III. Atomic positions of the fully-relaxed monoclinic structure with Cm space group corresponding to the unstable phonon mode at $(0, 0, \frac{1}{3})$. The lattice parameters are $a = 10.9416$, $b = 2.9232$, $c = 8.6562$ Å, $\alpha = 90^\circ$, $\beta = 119.8852^\circ$, and $\gamma = 98.8352^\circ$.

atom	x	y	z
Na	0.00026	0.00000	-0.00067
Na	0.33324	0.00000	0.66695
Na	0.66649	0.00000	0.33364
Ti	0.66982	0.00000	0.83891
Ti	-0.00500	0.00000	0.49110
Ti	0.33523	0.00000	0.17002
O	0.31661	0.00000	-0.08064
O	0.64591	0.00000	0.58974
O	-0.01538	0.00000	0.25265
O	0.02076	0.00000	0.74493
O	0.34856	0.00000	0.41536
O	0.68350	0.00000	0.07800